

# Population balance models for the thermal degradation of PMMA

J.E.J. Staggs

*Energy Resources Research Institute, University of Leeds, Leeds LS2 9JT, UK*

Received 4 December 2006; received in revised form 27 April 2007; accepted 27 April 2007

Available online 10 May 2007

---

## Abstract

A widely accepted view of the thermal degradation of polymers such as PMMA is that an initiation reaction produces radical fragments that undergo rapid depropagation and are also converted back to molecules by a termination reaction. This mechanism is applied to a population of linear molecules and radicals and the evolution of the population is modelled by appropriate discrete sets of ordinary differential equations. In particular, end-chain and random initiation reactions with first-order termination are analysed and compared with experimental data. We find on comparison with TG data for PMMA that the initiation reaction is important in dictating the qualitative behaviour of the overall rate of thermal degradation. Furthermore, the behaviour of degradation rate with initial degree of polymerisation is also investigated and interpreted within the framework of the model.

© 2007 Elsevier Ltd. All rights reserved.

*Keywords:* Thermal degradation; Population balance model; Random scission

---

## 1. Introduction

The population balance approach is a powerful modelling technique which describes the evolution of a population of linear molecules in terms of sets of ordinary or integro-partial differential equations (depending on whether the polymer molecule is viewed as a discrete number of repeat units linked with bonds or a continuous length which may be infinitely subdivided). In an earlier paper [1], the author presented a population balance model for discrete bond-weighted random scission of linear polymers. The model appeared to describe the thermal degradation of linear PE reasonably well, but was less successful when applied to PMMA. In particular, the observed variation of degradation rate with initial degree of polymerisation [2–5] was not correctly predicted at high temperatures. A widely accepted model for thermal degradation of linear polymers involves three processes: initiation, depropagation and termination [4–10]. The initiation reaction, where a polymer molecule undergoes scission at a random location or at an end bond, creates two radicals which undergo

rapid depropagation accompanied by a termination reaction where one or more radicals are converted into one or more molecules. This model, in a variety of forms, has previously been investigated using a variety of theoretical methods and simplifications [8–10]. The first attempts to analyse polymer degradation using population balance methods appear to have their origins in the 1950s and 1960s. Simha et al. [11] considered a degradation mechanism involving initiation, depropagation, inter- and intra-molecular transfer and second-order termination. In order to simplify the analysis, they assumed a mono-disperse initial distribution. Furthermore, they assumed that the radical concentration remains steady, thereby reducing the governing ordinary differential equations for radical species to algebraic difference equations. Boyd [12], whilst maintaining the steady radical assumption, extended this solution for a different initial molecular weight distribution and also considered different termination mechanisms such as first-order and recombination. He also considered the effect of volume change during degradation in a short letter [13]. All of these early approaches sought to predict the evolution of the molecular mass distribution, or some moment of it. More recently, the population balance method has been applied to the thermal degradation of a variety of

---

*E-mail address:* [j.e.j.staggs@leeds.ac.uk](mailto:j.e.j.staggs@leeds.ac.uk)

polymers using simplified mechanisms such as pure end-chain scission, pure random scission, recombination, combinations of these mechanisms or other more exotic (but not necessarily realistic) mechanisms [1,7–10,14–22].

In this paper a description based on the mechanisms postulated by Barlow et al. [2], Bagby et al. [3] and Lehrle et al. [4] is adopted. Here the inter- and intra-molecular hydrogen transfer reactions considered by Simha et al. [11], which have the overall effect of producing polymer molecules from radical fragments, are not explicitly included. Rather, a simple termination reaction is considered that converts radical fragments into polymer molecules. However, steady radical concentration is not assumed and the full population balance equations for initiation, depropagation and termination are considered and solved for a variety of different scenarios. The goals of this contribution are:

- To seek approximate solutions, where possible, to the model equations and provide a description of the overall degradation rate, where the initial polymer is converted into volatile species.
- To evaluate the influence of initiation mechanism both analytically and numerically on the overall degradation rate and to evaluate the relative effectiveness of the models in predicting the degradation behaviour of PMMA in thermogravimetric experiments.
- To provide insight into some of the observed thermal degradation behaviour of PMMA samples of differing initial degrees of polymerisation.

For brevity, only a single termination reaction is considered: first-order (where a radical fragment is converted directly into a polymer molecule of the same degree of polymerisation). However, the author plans to analyse the role of different termination mechanisms, such as recombination (where two radical fragments combine to produce a polymer molecule with degree of polymerisation equal to the sum of the degrees of polymerisation of the radical fragments) in a later paper. The choice of termination mechanism is in line with previous observations and analyses of the thermal degradation of PMMA and other polymers [4,6,10]. There does, however, seem to be some dispute in the literature over which mechanism most realistically represents termination for PMMA and other polymers. Lehrle et al. [4] discounted the possibility of second-order termination for polystyrene on the basis of derived values for activation energies. Inaba and Kashiwagi [8] state that, based on previous studies, only a first-order termination reaction can explain the degradation of PMMA. In a later paper, Lehrle et al. [6] essentially agree with this point, using their own kinetic data for PMMA. However, in earlier work Simha et al. [11] take the view that first-order termination is rare and consider only second-order termination. Boyd [12] does consider alternative termination reactions but does not comment on the relative merits of each.

We consider a discrete population of molecules where  $P_m$  denotes the ratio of the number of  $m$ -mers with  $m - 1$  links to the initial number of molecules and  $R_m$  denotes the

corresponding ratio for radicals with  $m - 1$  links. Degradation rate is quantified in terms of remaining mass and as in earlier papers [1,20–22], we take the simple view that species with fewer than  $m_v$  repeat units are volatile and are removed from the population as soon as they are formed. Accordingly, when considering the rate of formation of volatile species, the remaining mass is proportional to the first partial moment

$$\mu_{P+R}^{(m_v)}(\tau) = \sum_{i=m_v}^{\infty} i(P_i + R_i). \quad (1)$$

For simplicity, we shall consider only cases that evolve from an initially unimolecular distribution. Admittedly, this may not be relevant to common polymers which are manufactured with high degrees of polydispersity. However, the effects of polydispersity of the initial distribution on degradation rate and evolution of the molecular mass distributions are investigated numerically in later sections.

## 2. Initiation by end-chain scission, depropagation and first-order termination (ECS–D–O(1) model)

Here the initiation reaction, with rate term  $k_{ECS}$ , involves a polymer molecule breaking at an end bond, forming a polymer radical and a monomer radical:  $P_m \rightarrow R_{m-1} + R_1$ . A fast depropagation reaction, with rate term  $k_D$ , causes radical fragments to unzip forming monomer:  $R_m \rightarrow R_{m-1} + P_1$ . A termination reaction, with rate  $k_T$ , causes radical fragments to be converted back to polymer molecules:  $R_m \rightarrow P_m$ . Let  $\varepsilon_{ECS} = k_{ECS}/k_D$ ,  $\varepsilon_T = k_T/k_D$  and  $d\tau/dt = k_D$ . We assume that the depropagation reaction is faster than the initiation reaction, so  $\varepsilon_{ECS} < 1$ .

If  $n$  is the initial degree of polymerisation, then the corresponding population balance equations are

$$\frac{dP_m}{d\tau} = \begin{cases} \varepsilon_T R_1 + \sum_{j=2}^n R_j, & m = 1, \\ \varepsilon_T R_m - \varepsilon_{ECS} P_m, & 2 \leq m \leq n, \end{cases} \quad (2)$$

$$\frac{dR_m}{d\tau} = \begin{cases} -\varepsilon_T R_1 + R_2 + \varepsilon_{ECS}(P_2 + \sum_{j=2}^n P_j), & m = 1, \\ -(1 + \varepsilon_T)R_m + R_{m+1} + \varepsilon_{ECS}P_{m+1}, & 2 \leq m < n. \end{cases} \quad (3)$$

When  $m = n$ , no radical fragments can be formed as there are no  $(n + 1)$ -mers and so  $R_n = 0$  for all  $\tau$ .

### 2.1. Solution for very rapid depropagation

When the depropagation reaction is much faster than the termination reaction we may set  $\varepsilon_T = 0$ . For a unimolecular initial distribution of polymer molecules, where  $P_n(0) = 1$ ,  $P_m(0) = 0$ ,  $1 \leq m \leq n - 1$ , it may be shown that the solution of the population balance equations takes the form

$$\left. \begin{aligned} P_n(\tau) &= e^{-\varepsilon_{ECS}\tau}, \quad P_m(\tau) = 0, \quad 2 \leq m \leq n - 1, \\ R_m(\tau) &= \frac{\varepsilon_{ECS} e^{-\tau}}{(1 - \varepsilon_{ECS})^{n-m}} \sum_{j=n-m}^{\infty} \frac{(1 - \varepsilon_{ECS})^j \tau^j}{j!}, \quad 2 \leq m \leq n - 1 \end{aligned} \right\} \quad (4)$$

Also, if  $n\varepsilon_{\text{ECS}}$  is not small compared with 1, it may be shown that  $R - R_1 = \sum_{m=2}^n R_m \approx 1 - \exp(-\varepsilon_{\text{ECS}}\tau)$ . Consequently, the remaining mass (assuming that the only volatile species are monomers) will be given approximately by

$$\frac{\mu_{P+R}^{(2)}(\tau)}{\mu_{P+R}^{(2)}(0)} \approx 1 - \frac{\tau}{n} + \frac{1 - \varepsilon_{\text{ECS}}}{n\varepsilon_{\text{ECS}}}(1 - e^{-\varepsilon_{\text{ECS}}\tau}). \quad (5)$$

As the depropagation rate increases and  $\varepsilon_{\text{ECS}}$  gets very small, it follows that any radicals will be instantaneously converted into monomer units and the availability of radicals will be dominated by the end-chain initiation rate. Therefore, for very small  $\varepsilon_{\text{ECS}}$ , expression (5) above for remaining mass will become increasingly invalid for large  $\tau$  and a better approximation will be given by

$$\frac{\mu_{P+R}^{(2)}(\tau)}{\mu_{P+R}^{(2)}(0)} \approx e^{-\varepsilon_{\text{ECS}}\tau}. \quad (6)$$

It is possible to construct a uniformly valid approximation for the remaining mass using expressions (5) and (6). Expression (5) is used for  $\tau < \tau_0$  and the expression  $Ae^{-\varepsilon_{\text{ECS}}\tau}$  when  $\tau \geq \tau_0$ . The constants  $A$  and  $\tau_0$  are found from the conditions that the slopes of the two expressions are identical and the remaining mass is continuous at  $\tau = \tau_0$ . It transpires that  $\tau_0 = n$  and

$$A = \left( \frac{1 - \varepsilon_{\text{ECS}}}{n\varepsilon_{\text{ECS}}} \right) (e^{n\varepsilon_{\text{ECS}}} - 1). \quad (7)$$

Hence the final expression for remaining mass is

$$\frac{\mu_{P+R}^{(2)}(\tau)}{\mu_{P+R}^{(2)}(0)} \approx \begin{cases} 1 - \frac{\tau}{n} + \left( \frac{1 - \varepsilon_{\text{ECS}}}{n\varepsilon_{\text{ECS}}} \right) (1 - e^{-\varepsilon_{\text{ECS}}\tau}), & \tau < n, \\ \left( \frac{1 - \varepsilon_{\text{ECS}}}{n\varepsilon_{\text{ECS}}} \right) (e^{-\varepsilon_{\text{ECS}}(\tau-n)} - e^{-\varepsilon_{\text{ECS}}\tau}), & \tau \geq n. \end{cases} \quad (8)$$

The graph in Fig. 1 illustrates the excellent agreement between the approximate expression for remaining mass (8)

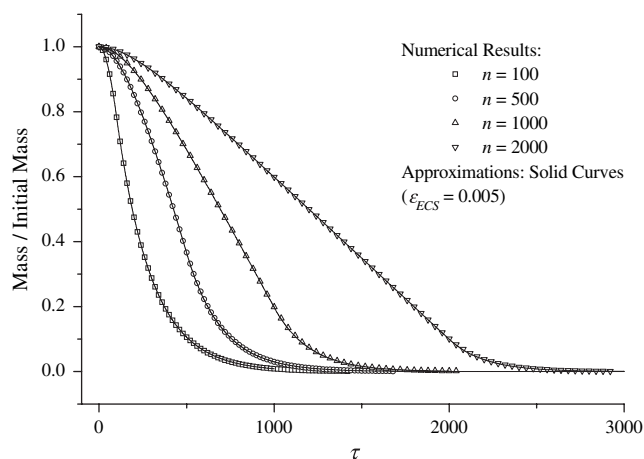


Fig. 1. Comparison between approximate and numerical results for slow termination ( $\varepsilon_{\text{ECS}} = 0.005$ ,  $\varepsilon_{\text{T}} = 0$ ).

above and numerical results for  $\varepsilon_{\text{ECS}} = 0.005$  and a range of values of  $n$ .

## 2.2. Effect of termination

The numerical results in Fig. 2 show the effect of termination on the degradation rate for  $\varepsilon_{\text{ECS}} = 0.1$ . As the termination reaction rate increases, fewer radical fragments are available for depropagation and so the rate of production of monomers falls, thereby lowering the overall rate of degradation. As the termination rate becomes very large, radical fragments are instantaneously converted back to polymer molecules and so the system becomes governed by the equations  $dP_m/d\tau = \varepsilon_{\text{ECS}}(P_{m+1} - P_m)$ ,  $2 \leq m < n$ , which represent a simple model for pure ECS that has been studied in detail in earlier papers [21]. It is relatively easy to show for this model that the remaining mass is given to a good approximation by

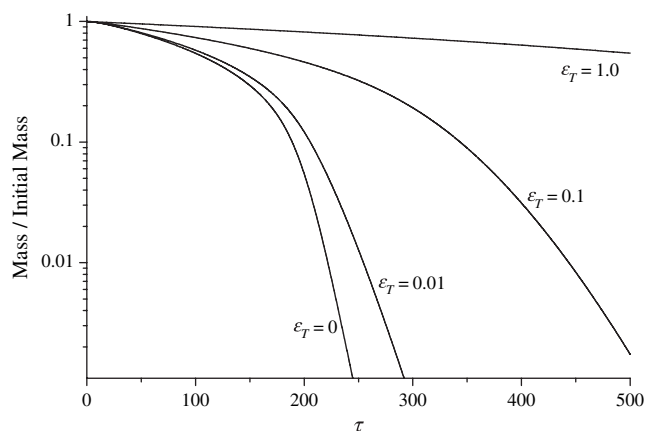


Fig. 2. Effect of termination for ECS initiation ( $k_{\text{ECS}}/k_{\text{D}} = 0.1$ ,  $n = 200$ ).

$$\frac{\mu_{P+R}^{(2)}(\tau)}{\mu_{P+R}^{(2)}(0)} = 1 - \frac{\varepsilon_{\text{ECS}}\tau}{n}. \quad (9)$$

## 2.3. Effect of initial molecular mass distribution

All of the theoretical solutions presented in Section 2 above were computed assuming a unimolecular initial distribution (UID) for the polymer molecules. It has been demonstrated in an earlier paper [21] that for pure ECS, the shape of the initial distribution has no effect on the mass loss rate. However, this may no longer be the case in the present model and this is now briefly investigated.

The graphs in Fig. 3 show the effect on the mass loss rate and relative frequency of polymer molecules for normally distributed initial populations with means located at  $m = 400$  and various values of standard deviation  $\sigma$ . The graphs correspond to the parameter values  $k_{\text{ECS}}/k_{\text{D}} = 0.1$ ,  $k_{\text{T}}/k_{\text{D}} = 0.1$ . Note that as  $\sigma$  is varied there is a large effect on the evolution of the population distribution, however, there is only a low order effect on the evolution rate of monomer species and hence on mass loss rate.

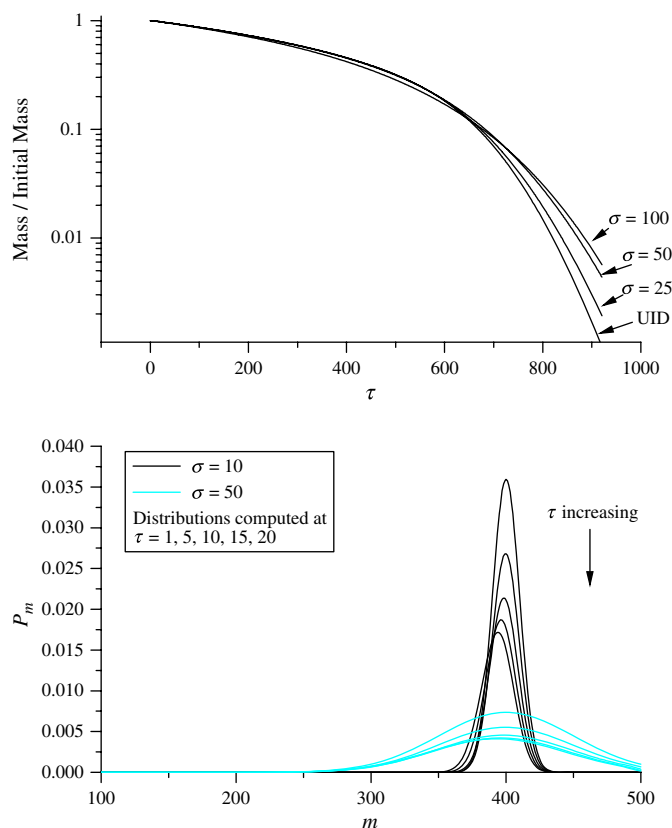


Fig. 3. Effect of the shape of the initial distribution for ECS–D–O(1) model on mass loss rate (top) and population of polymer molecules (bottom).

#### 2.4. Comparison with TG experiments

When compared to experimental TG curves, the ECS–D–O(1) model shows poor agreement. In fact not even the qualitative nature of the mass loss curves is reproduced. The graph in Fig. 4 shows the results of an attempt to fit the model to two isothermal TG mass loss curves. The TG experiments were carried out in nitrogen on PMMA samples of initial molecular weight  $49,600 \text{ g mol}^{-1}$  and low polydispersity of 1.02

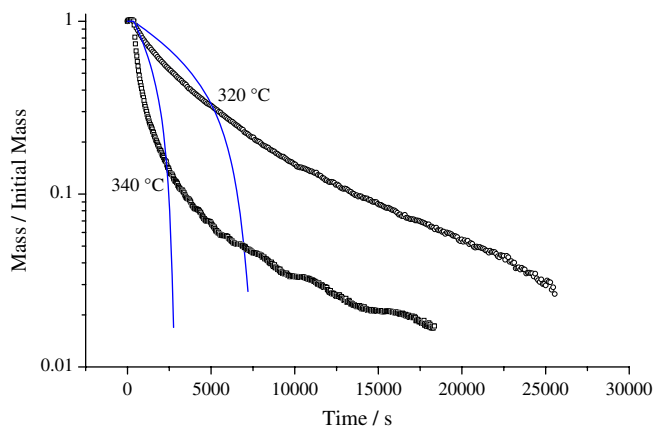


Fig. 4. Comparison with isothermal TG experiments: solid curves are model predictions and symbols are experimental results.

(corresponding to a standard deviation of  $\sigma = 70$ ), so that the experimental results may be compared with model solutions obtained from UID. The polymer samples were obtained from Polymer Laboratories (UK) Inc. (part no. 2023-3001, batch no. 20233-11) and the PMMA molecules were terminated by diphenyl hexyl units. Since each end-chain initiation event generates a monomer and a radical, which itself rapidly depropagates, as lower molecular mass species are generated, the rate of evolution of monomers increases as shown by the curves in Fig. 2. The effect of increasing the rate of termination makes fewer radicals available for depropagation and hence the mass loss rate is slowed (assuming that depropagation is much faster than initiation). The experimental data show that the rate of mass loss actually decreases as time increases – a feature that cannot be predicted by the end-chain initiation model with first-order termination.

### 3. Initiation by random scission, depropagation and first-order termination (RS–D–O(1) model)

Here the initiation reaction, with rate term  $k_{RS}$ , involves a polymer molecule breaking at a random bond along the length of the molecule, forming two polymer radicals:  $P_m \rightarrow R_{m-r} + R_r$ . As above, a fast depropagation reaction, with rate term  $k_D$ , causes radical fragments to unzip forming monomers:  $R_m \rightarrow R_{m-1} + P_1$ . A termination reaction, with rate  $k_T$ , causes radical fragments to be converted back to polymer molecules:  $R_m \rightarrow P_m$ . Let  $\varepsilon_{RS} = k_{RS}/k_D$ ,  $\varepsilon_T = k_T/k_D$ , then with  $\tau$  and  $n$  defined as before, the population balance equations are

$$\frac{dP_m}{d\tau} = \begin{cases} \varepsilon_T R_1 + \sum_{j=2}^n R_j, & m = 1, \\ \varepsilon_T R_m - \varepsilon_{RS}(m-1)P_m, & 2 \leq m \leq n, \end{cases} \quad (10)$$

$$\frac{dR_m}{d\tau} = \begin{cases} -\varepsilon_T R_1 + R_2 + 2\varepsilon_{RS} \sum_{j=2}^n P_j, & m = 1, \\ -(1 + \varepsilon_T)R_m + R_{m+1} + 2\varepsilon_{RS} \sum_{j=m+1}^n P_j, & 2 \leq m < n. \end{cases} \quad (11)$$

When  $m = n$ , no radical fragments can be formed as there are no  $(n+1)$ -mers and so  $R_n = 0$  for all  $\tau$ .

#### 3.1. Solution for very rapid depropagation

As before, when the depropagation reaction is much faster than the termination reaction we may set  $\varepsilon_T = 0$ . Now, for a uniform initial distribution, it follows that  $P_n(\tau) = e^{-\varepsilon_{RS}(n-1)\tau}$ ,  $P_m(\tau) = 0$ ,  $2 \leq m \leq n-1$ . Also, it may be shown that

$$R_m = \frac{2}{n-1} (1 - e^{-\varepsilon_{RS}(n-1)\tau}), \quad m > 1, \quad (12)$$

is a solution for the radical population valid when  $\varepsilon_{RS}(m-1)\tau \gg 1$ . This approximation is illustrated by the graph in Fig. 5. Here numerical solutions for the radical

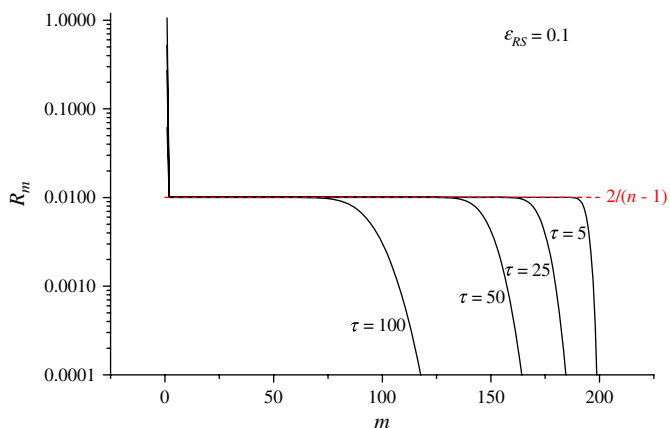


Fig. 5. Frequency of radicals for  $\epsilon_{RS} = 0.1$ ,  $n = 200$ .

frequencies  $R_m$  are plotted at  $\tau = 5, 25, 50, 100$  for  $\epsilon_{RS} = 0.1$ , together with the line  $2/(n - 1)$ .

Using this result, it follows from the population balance equations that

$$R_1 \approx \frac{2\tau}{n - 1}, \quad P_1 \approx 2\tau - \frac{\tau^2}{n - 1}, \quad (13)$$

and so the remaining mass (assuming that the only volatile species are monomers) will be given approximately by

$$\frac{\mu_{P+R}^{(2)}(\tau)}{\mu_{P+R}^{(2)}(0)} \approx 1 - \frac{2\tau}{n} \left( 1 - \frac{\tau}{2(n - 1)} \right). \quad (14)$$

This expression is a good approximation for the remaining mass provided that  $\epsilon_{RS}(n - 1)$  is not small. When this is the case, it may be shown that the remaining mass (when  $\epsilon_{RS}(n - 1)\tau$  is not too large) is given by

$$\frac{\mu_{P+R}^{(2)}(\tau)}{\mu_{P+R}^{(2)}(0)} \approx 1 - \lambda \left( \tau - \frac{1 - e^{-\epsilon_{RS}(n-1)\tau}}{\epsilon_{RS}(n-1)} \right) + \frac{\tau^2}{n(n-1)}, \quad (15)$$

where the constant  $\lambda$  is given by

$$\lambda = \frac{2}{n} \left( 1 + \frac{1}{n-1} + \frac{1}{\epsilon_{RS}(n-1)^2} \right). \quad (16)$$

As  $\epsilon_{RS}(n - 1)$  becomes very small, as in the case of end-chain initiation, the behaviour will be governed by the rate of random scission, and so a better expression for the remaining mass will be proportional to  $\exp(-\epsilon_{RS}(n - 1)\tau)$ . Now, using this observation and expression (15) above, it is possible to construct a uniformly valid approximation for remaining mass for all  $\tau$  and small  $\epsilon_{RS}$ . Accordingly, we use expression (15) for  $\tau < \tau_1$  and the expression  $B\exp(-\epsilon_{RS}(n - 1)\tau)$  when  $\tau \geq \tau_1$ . The constants  $B$  and  $\tau_1$  are found from the conditions that the slopes of the two expressions are identical and the remaining mass is continuous at  $\tau = \tau_1$ . Using these conditions, it transpires that

$$\tau_1 = n - \sqrt{n}, \quad B = \lambda \left( \frac{e^{\epsilon_{RS}(n-1)\tau_1} - 1}{\epsilon_{RS}(n-1)} \right) - \frac{2\tau_1 e^{\epsilon_{RS}(n-1)\tau_1}}{\epsilon_{RS}n(n-1)^2}. \quad (17)$$

Hence the final approximation for remaining mass, valid for small  $\epsilon_{RS}$ , is given by

$$\frac{\mu_{P+R}^{(2)}(\tau)}{\mu_{P+R}^{(2)}(0)} \approx \begin{cases} 1 - \lambda \left( \tau - \frac{1 - e^{-\epsilon_{RS}(n-1)\tau}}{\epsilon_{RS}(n-1)} \right) + \frac{\tau^2}{n(n-1)}, & \tau < \tau_1, \\ \lambda \left( \frac{e^{-\epsilon_{RS}(n-1)(\tau-\tau_1)} - e^{-\epsilon_{RS}(n-1)\tau}}{\epsilon_{RS}(n-1)} \right) - \frac{2\tau_1 e^{-\epsilon_{RS}(n-1)(\tau-\tau_1)}}{\epsilon_{RS}n(n-1)^2}, & \tau \geq \tau_1. \end{cases} \quad (18)$$

Inspection of numerical results suggests that when  $\epsilon_{RS}(n - 1) > 0.1$ , approximation (14) may be used, otherwise approximation (18) is valid. The two approximations are compared with numerical results in Fig. 6 for  $n = 200$ . Approximation (18) was used for  $\epsilon_{RS} = 0.0001, 0.00025$  and approximation (14) was used for  $\epsilon_{RS} = 0.01$ . When  $\epsilon_{RS} > 0.0005$ , the numerical results (not shown in Fig. 6) are indistinguishable from those for  $\epsilon_{RS} = 0.01$ .

### 3.2. Effect of termination

Again, as in the case of end-chain initiation above, as the termination rate becomes very large, radical fragments are instantaneously converted back to polymer molecules and so the system becomes governed by the equations  $dP_m/d\tau = -\epsilon_{RS}(m - 1)P_m + 2\epsilon_{ECS} \sum_{j=m+1}^n P_j$ ,  $2 \leq m < n$ , which represent a simple model for pure RS that has been studied in detail in earlier papers [1,20,22]. For this model, it is possible to show that the remaining mass (assuming that the only volatile species are monomers) is given by

$$\frac{\mu_{P+R}^{(2)}(\tau)}{\mu_{P+R}^{(2)}(0)} = 2 \left( 1 - \frac{1}{n} \right) e^{-\epsilon_{RS}\tau} - \left( 1 - \frac{2}{n} \right) e^{-2\epsilon_{RS}\tau}. \quad (19)$$

The effect of finite termination rate on the mass loss rate is shown by the numerical solutions in Fig. 7. Here the remaining

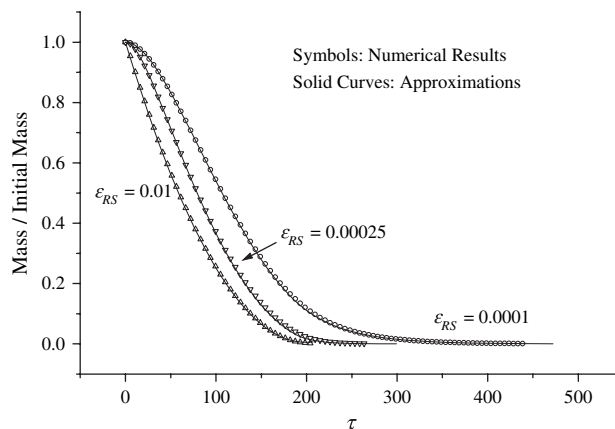


Fig. 6. Comparison between numerical results and approximate results for random initiation with very slow termination ( $k_T/k_D = 0$ ,  $n = 200$ ).

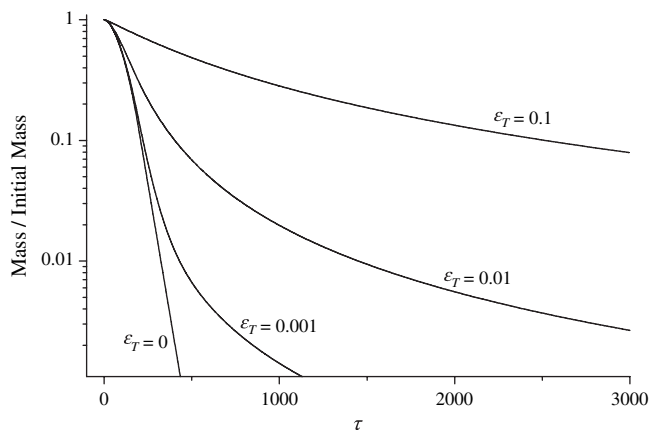


Fig. 7. Effect of termination for random initiation ( $k_{RS}/k_D = 0.0001$ ,  $n = 200$ ).

mass is plotted as a function of  $\tau$  for  $\epsilon_{RS} = 0.0001$ ,  $n = 200$  and  $\epsilon_T = 0, 0.001, 0.01, 0.1$ . Again as the rate of termination increases, fewer radicals are available for fast depropagation and so the overall rate of mass loss reduces. However, an interesting additional feature also develops. When the rate of termination is non-zero, radicals are converted back into molecules which must undergo an initiation reaction which now depends on the size of the molecule – the rate of random scission for an  $m$ -mer is  $(m - 1)k_{RS}$ . Consequently, as lower molecular mass species are produced, the overall rate of random scissions also reduces, conspiring to reduce the rate of monomer production and hence the rate of mass loss.

Fig. 8 shows the effect of finite termination rate on the radical distribution at different times for  $k_{RS}/k_D = 0.0001$ ,  $k_T/k_D = 0.01$ ,  $n = 200$ . These results show that the assumption of steady radical concentration is not valid for even small termination rates.

### 3.3. Effect of initial molecular mass distribution

All of the theoretical solutions presented in Section 3 above were computed assuming a unimolecular initial distribution

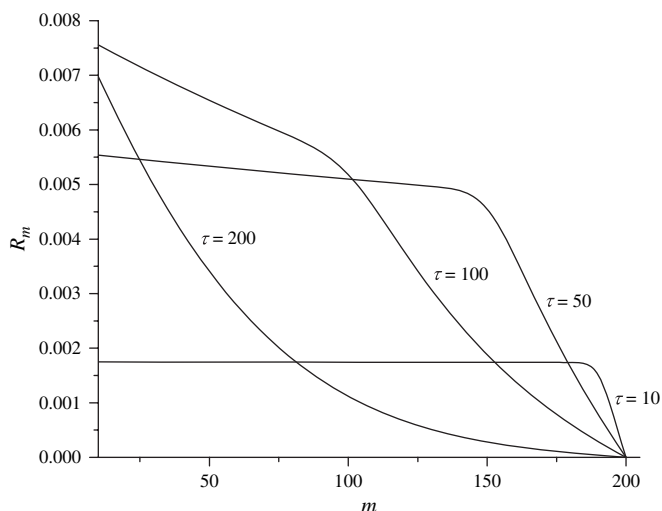


Fig. 8. Dependence of radical concentration on time ( $k_{RS}/k_D = 0.0001$ ,  $k_T/k_D = 0.01$ ,  $n = 200$ ).

(UID) for the polymer molecules. It has been demonstrated in an earlier paper [1] that for pure random scission, the shape of the initial distribution has no effect on the mass loss rate. We now briefly investigate the effect of the shape of the initial distribution on mass loss rate.

The graphs in Fig. 9 show the effect on the mass loss rate (expressed as a percentage relative difference from the corresponding mass loss rate for a UID) and relative frequency of polymer molecules for normally distributed initial populations with means located at  $m = 400$  and various values of standard deviation  $\sigma$  (a polydispersity of 1.02, as in the PMMA samples used for comparison above, corresponds to  $\sigma = 70$ ). The graphs correspond to the parameter values  $k_{RS}/k_D = 0.00001$ ,  $k_T/k_D = 0.25$ . Note that despite the fact that as  $\sigma$  is varied there is a large effect on the evolution of the population distribution, there is very little effect on the evolution rate of monomer species and hence on mass loss rate.

### 3.4. Comparison with TG experiments

On comparison with experimental TG curves, it appears that kinetic parameters may be found by a least squares fitting process such that the RS–D–O(1) model reproduces the observed mass loss behaviour for the PMMA samples used in the previous section. The graph in Fig. 10 shows the results of a least squares fit to two isothermal TG curves. The kinetic parameters of best fit are shown in Table 1, assuming that each rate term is of Arrhenius form  $k(T) = A \exp(-T_A/T)$ .

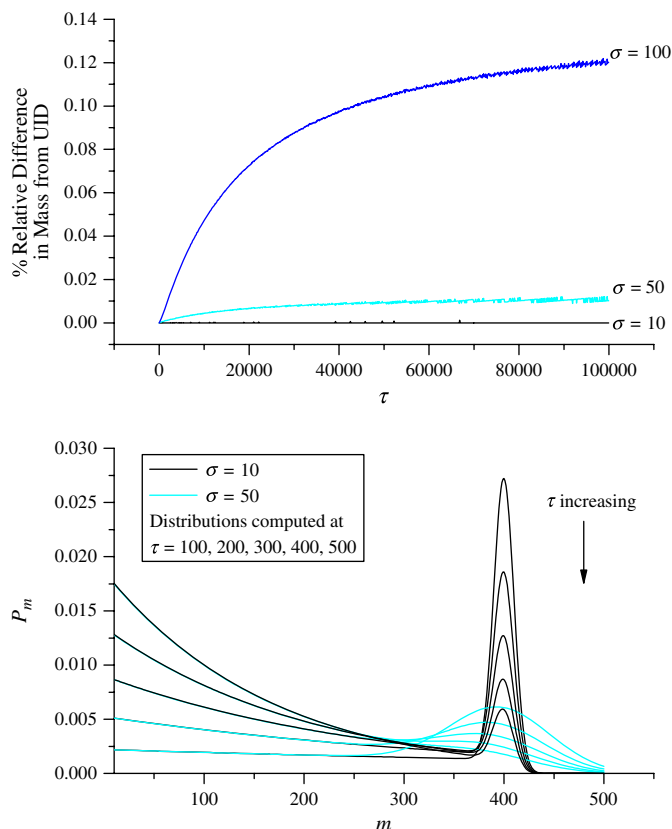


Fig. 9. Effect of the shape of the initial distribution RS–D–O(1) model on mass loss rate (top) and population of polymer molecules (bottom).

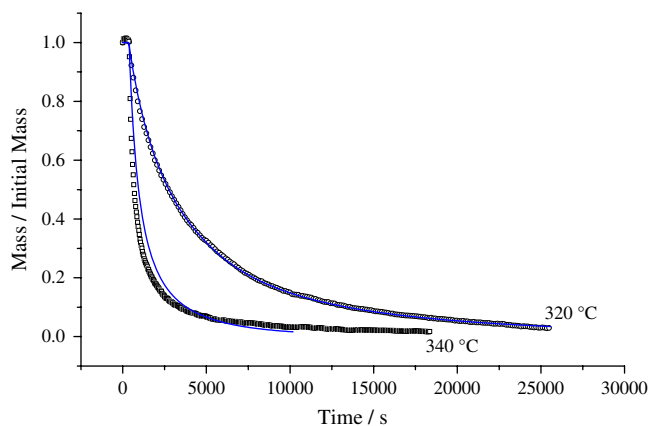


Fig. 10. Comparison with isothermal TG experiments: solid curves are model predictions and symbols are experimental results.

Fig. 11 shows model predictions compared to constant heating rate TG experiments (over the first 90% of mass loss) for the same sample of PMMA, using the parameter values in Table 1. Again the model shows excellent agreement with experiment. It should be noted that nothing has been proved about the uniqueness of this fit and that there may be other parameter values which give better results. Also, one should not be precipitate in drawing conclusions about the actual rate terms for initiation, depropagation and termination based on these kinetic parameters for the same reason.

### 3.5. Variation of degradation rate with initial degree of polymerisation

In previous studies on the thermal degradation of PMMA [2–5], attempts have been made to interpret aspects of the

Table 1  
Kinetic parameters of best fit for model 2

	$A/s^{-1}$	$T_A/K$
$k_{RS}$	$6.172 \times 10^{11}$	21885.22
$k_D$	$1.789 \times 10^{16}$	21114.63
$k_T$	$2.850 \times 10^{13}$	18000.39

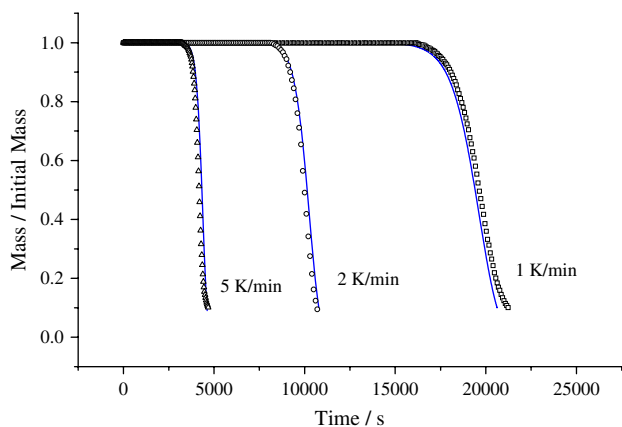


Fig. 11. Comparison with constant heating rate TG experiments: solid curves are model predictions and symbols are experimental results.

degradation mechanism in terms of the dependence of degradation rate  $k_{obs}$  on initial degree of polymerisation  $n$ . In these approaches, it is assumed that the initial degradation behaviour is first-order and consequently the remaining mass varies with time according to  $\exp(-k_{obs}t)$ . A value for  $k_{obs}$  is then found from a log plot of an initial portion of the remaining mass, or some other similar procedure. Whereas this is a perfectly acceptable way of characterising the degradation behaviour, it presupposes a relationship which may not be valid. Instead, a different metric is employed here. Let  $t_{1/2}$  denote the time taken for 50% of the initial mass to volatilise. Then we define our characteristic degradation rate  $k_{1/2} = 1/t_{1/2}$ . When remaining mass varies according to  $\exp(-k_{obs}t)$ , there is a simple relationship between  $k_{1/2}$  and  $k_{obs}$ , viz  $k_{1/2} = k_{obs}/\ln 2$ .

For the case of infinitely rapid termination, it may be shown that for large initial degree of polymerisation  $n$ ,  $k_{1/2} \sim 0.814k_{RS}(1 + 0.814/n)$ , indicating that  $k_{1/2}$  increases with  $1/n$ . However, when the rate of termination is finite, this is not always the case as Fig. 12 shows. Here we see calculations of  $k_{1/2}$  for different values of  $\epsilon_{RS}$  and  $\epsilon_T$  as functions of  $1/n$ . For  $\epsilon_{RS} = 0.0001$  the general trend is for  $k_{1/2}$  to increase with  $1/n$ , with the overall rate decreasing as  $\epsilon_T$  increases. However, when  $\epsilon_{RS} = 5 \times 10^{-6}$ , the general trend (with the exception of  $\epsilon_T = 0.01$  which has a maximum) is for  $k_{1/2}$  to reduce with  $1/n$ , again with the overall rate decreasing as  $\epsilon_T$  increases.

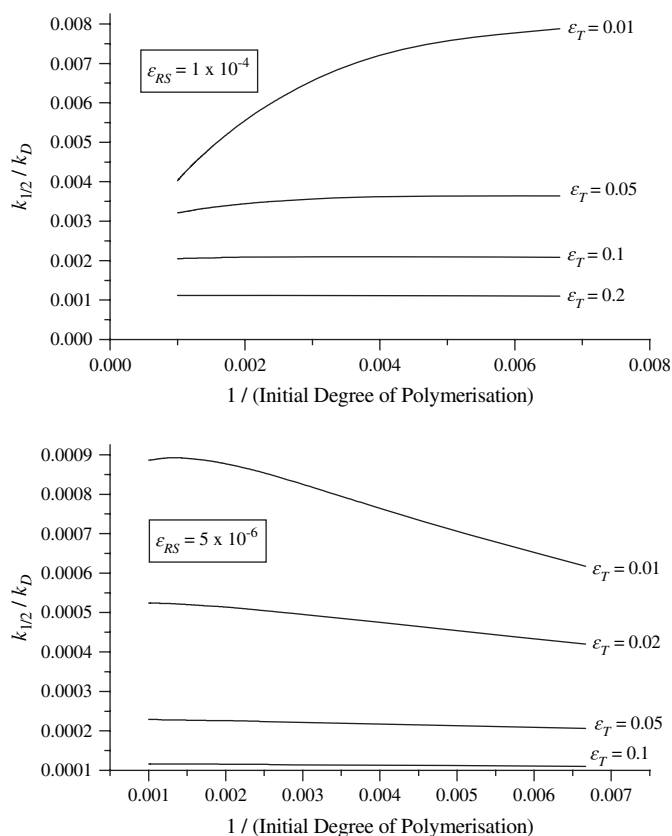


Fig. 12. Variation of  $k_{1/2}$  with initial degree of polymerisation.

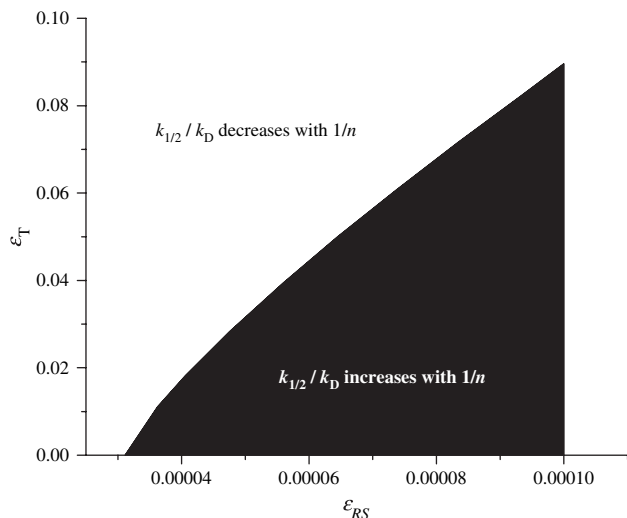


Fig. 13. Dependence of  $k_{1/2}$  on  $1/n$  as a function of termination and random scission rates.

This behaviour is investigated numerically in greater detail in Fig. 13. This figure shows the results of computing values of  $d(k_{1/2}/k_D)/dn$  at  $1/n=0.004$ . The region where  $d(k_{1/2}/k_D)/dn < 0$  corresponds to the region where  $k_{1/2}/k_D$  increases with  $1/n$  and is filled black in the figure. Further analysis of the data in Fig. 13 indicates that the change of sign of  $d(k_{1/2}/k_D)/dn$  occurs along the curve given to a good approximation by  $\epsilon_T = 191.43(\epsilon_{RS} - 3.12 \times 10^{-5})^{0.8}$ .

This figure clearly shows that either increasing the termination rate or decreasing the random scission rate will have the effect of changing the behaviour of  $k_{1/2}$  as a function of  $1/n$  from increasing to decreasing. Previous experimental studies [1,2–5] have shown that the behaviour of  $k_{obs}$  with  $1/n$  tends to move from monotonic increasing to monotonic decreasing as temperature increases. Within the framework of the random initiation model, the most likely explanation of this observation is probably given by one of the following:

1. As temperature increases, the relative rate of depropagation to random scission increases, whilst the relative rate of termination to depropagation remains approximately constant, does not reduce rapidly or increases.
2. As temperature increases, the relative rate of termination to depropagation increases, whilst the relative rate of depropagation to random initiation remains approximately constant, does not reduce rapidly or increases.

#### 4. Combined end-chain and random scission, infinitely rapid termination

While not necessarily relevant to the thermal degradation of PMMA, this case is included because it admits an exact solution for large initial degree of polymerisation. As the rate of termination becomes very large, radical fragments formed from end-chain and random scission initiation reactions will be instantaneously converted back into polymer molecules

and the depropagation reaction will not have time to take place. Under these conditions, the population balance equations reduce to

$$\frac{dP_m}{d\tau} = \begin{cases} \epsilon_{ECS}P_2 + (\epsilon_{ECS} + 2\epsilon_{RS})\sum_{j=2}^n P_j, & m = 1, \\ -\{\epsilon_{ECS} + \epsilon_{RS}(m-1)\}P_m + \epsilon_{ECS}P_{m+1} \\ \quad + 2\epsilon_{RS}\sum_{j=m+1}^n P_j, & 2 \leq m, \\ -\{\epsilon_{ECS} + \epsilon_{RS}(n-1)\}P_n, & m = n. \end{cases} \quad (20)$$

We therefore essentially recover the simpler case of a population of molecules undergoing simultaneous random and end-chain scission. Now, for a uniform initial distribution with initially large degree of polymerisation ( $n \rightarrow \infty$ ), it can be shown by direct substitution that the solutions of these equations for  $m > 1$  are

$$\frac{P_m(\tau)}{\mu_p} = \exp\left\{-[\epsilon_{ECS} + \epsilon_{RS}(m-1)]\tau + \frac{\epsilon_{ECS}}{\epsilon_{RS}}(1 - e^{-\epsilon_{RS}\tau})\right\} \times (1 - e^{-\epsilon_{RS}\tau})^2, \quad (21)$$

with the remaining mass being given by

$$\frac{\mu_p^{(m_v)}(\tau)}{\mu_p^{(m_v)}(0)} = \exp\left\{-[\epsilon_{ECS} + \epsilon_{RS}(m_v-1)]\tau + \frac{\epsilon_{ECS}}{\epsilon_{RS}}(1 - e^{-\epsilon_{RS}\tau})\right\} \times \{m_v - (m_v - 1)e^{-\epsilon_{RS}\tau}\}. \quad (22)$$

## 5. Conclusion

The use of discrete population balance equations, applied to the initiation–depropagation–termination degradation scheme, to investigate and interpret the thermal degradation of PMMA has produced interesting results. Whereas this approach has been investigated by others previously using similar population balance models, new light is shed by this work on the influence of the initiation reaction on the observed degradation rate.

Analytical approximations for end-chain and random initiation, valid when the depropagation rate is much faster than termination, have been derived for unimolecular initial distributions and compare well with numerical solutions. Also the case of pure end-chain scission combined with random scission with infinitely rapid termination has been shown to admit an exact solution valid for large initial degree of polymerisation.

Numerical results show that end-chain initiation with first-order termination does not reproduce the qualitative behaviour of PMMA in isothermal TG experiments. Further calculations show that random initiation with first-order termination is a much better candidate and both isothermal and constant heating rate TG results agree well with numerical results. Furthermore, numerical results show that the shape of the initial



molecular mass distribution has only a small effect on mass loss rate for both types of initiation reaction. This suggests that the simplification of adopting a unimolecular initial distribution is not critical when predicting mass loss rate. The dependence of observed degradation rate  $k_{\text{obs}}$  on initial degree of polymerisation for random initiation has also been investigated using detailed numerical calculations. It was found that the population balance model predicts that for small values of random initiation (random initiation rate/depropagation rate  $< 3.12 \times 10^{-5}$ ),  $k_{\text{obs}}$  always decreases as a function of  $1/(\text{initial degree of polymerisation})$  for termination rate/depropagation rate  $< 0.1$ . However, for values of random initiation rate/depropagation rate  $> 3.12 \times 10^{-5}$ , as the ratio of first-order termination to depropagation rate decreases, or as the ratio of random initiation to depropagation increases, the behaviour of  $k_{\text{obs}}$  will change to an increasing function of  $1/(\text{initial degree of polymerisation})$ .

## References

- [1] Staggs JEJ. Discrete bond-weighted random scission of linear polymers. *Polymer* 2006;47:897.
- [2] Barlow A, Lehrle RS, Robb JC, Sunderland D. Polymethylmethacrylate degradation — kinetics and mechanisms in the temperature range 340 to 460 °C. *Polymer* 1967;2:527.
- [3] Bagby G, Lehrle RS, Robb JC. Kinetic measurements by micropyrolysis—GLC: thermal degradation of polymethylmethacrylate possessing lauryl—mercaptyl end groups. *Polymer* 1969;10:683.
- [4] Lehrle RS, Peakman RE, Robb JC. Pyrolysis—gas—liquid—chromatography utilised for a kinetic study of the mechanisms of initiation and termination in the thermal degradation of polystyrene. *European Polymer Journal* 1982;18:529.
- [5] Holland BJ, Hay JN. The kinetics and mechanisms of the thermal degradation of poly(methyl methacrylate) studied by thermal analysis—Fourier transform infrared spectroscopy. *Polymer* 2001;42:4825.
- [6] Lehrle RS, Atkinson D, Cook S, Gardner P, Groves S, Hancox R, et al. Polymer degradation mechanisms: new approaches. *Polymer Degradation and Stability* 1993;42:281.
- [7] Kashiwagi T, Inaba A, Brown JE, Hatada K, Kitayama T, Masuda E. Effects of weak linkages on the thermal and oxidative degradation of poly(methyl methacrylates). *Macromolecules* 1986;19:2160.
- [8] Inaba A, Kashiwagi T. A calculation of thermal degradation initiated by random scission. I. Steady state radical concentration. *Macromolecules* 1986;19:2412.
- [9] Inaba A, Kashiwagi T. A calculation of thermal degradation initiated by random scission. II. Unsteady state radical concentration. *European Polymer Journal* 1987;23:871.
- [10] Inaba A, Kashiwagi T, Brown JE. Effects of initial molecular weight on thermal degradation of poly(methyl methacrylate): Part 1 — Model 1. *Polymer Degradation and Stability* 1988;21:1.
- [11] Simha R, Wall LA, Blatz J. Depolymerisation as a chain reaction. *Journal of Polymer Science* 1950;5:615.
- [12] Boyd RH. Theoretical depolymerization kinetics in polymers having an initial “most probable” molecular weight distribution. *Journal of Chemical Physics* 1959;31:321.
- [13] Boyd RH. The effect of changing volume in the kinetics of bulk polymer degradation. *Journal of Polymer Science* 1961;49:S1.
- [14] McCoy BJ, Madras G. Evolution to similarity solutions for fragmentation and aggregation. *Journal of Colloid and Interface Science* 1998;201:200.
- [15] McCoy B. Distribution kinetics for temperature-programmed pyrolysis. *Industrial and Engineering Chemistry Research* 1999;38:4531.
- [16] McCoy B. Polymer thermogravimetric analysis: effects of chain-end and reversible random scission. *Chemical Engineering Science* 2001;56:1525.
- [17] McCoy BJ, Madras G. Discrete and continuous models for polymerization and depolymerization. *Chemical Engineering Science* 2001;56:2831.
- [18] Madras G, McCoy B. Numerical and similarity solutions for reversible population balance equations with size-dependent rates. *Journal of Colloid and Interface Science* 2002;246:356.
- [19] Kostoglou M. Mathematical analysis of polymer degradation with end-chain scission. *Chemical Engineering Science* 2000;55:2507.
- [20] Staggs JEJ. Modelling random scission of linear polymers. *Polymer Degradation and Stability* 2002;76:37.
- [21] Staggs JEJ. Modelling end-chain scission and recombination of linear polymers. *Polymer Degradation and Stability* 2004;85:759.
- [22] Staggs JEJ. A continuous model for vaporisation of linear polymers by random scission and recombination. *Fire Safety Journal* 2005;40:610.